Chemistry & Biology
Brief Communication

Redesign of a Dioxygenase in Morphine Biosynthesis

Weerawat Runguphan,[1,4,5] Weslee S. Glenn,[1,2,4] and Sarah E. O'Connor[2,3,*]
[1]Department of Chemistry, Massachusetts Institute of Technology, Cambridge, MA 02139, USA
[2]Department of Biological Chemistry, The John Innes Centre, Norwich Research Park, Norwich NR4 7UH, UK
[3]School of Chemistry, The University of East Anglia, Norwich Research Park, Norwich NR4 7TJ, UK
[4]These authors contributed equally to this work
[5]Present address: Joint BioEnergy Institute, 5885 Hollis Street, Emeryville, CA 94608, USA
*Correspondence: sarah.o'connor@jic.ac.uk
DOI 10.1016/j.chembiol.2012.04.017

SUMMARY

Opium poppy (*Papaver somniferum*) produces medicinally important benzylisoquinoline alkaloids, including the analgesics codeine and morphine, in the morphinan pathway. We aligned three dioxygenases that were recently discovered in *P. somniferum* and subsequently identified the nonconserved regions. Two of these enzymes, codeine O-demethylase (*Ps*CODM) and thebaine O-demethylase (*Ps*T6ODM), are known to facilitate regioselective O-demethylation in morphinan biosynthesis. We systematically swapped the residues that were nonconserved between the *Ps*CODM and *Ps*T6ODM sequences to generate 16 mutant *Ps*CODM proteins that could be overexpressed in *Escherichia coli*. While wild-type *Ps*CODM can demethylate both codeine and thebaine, one engineered *Ps*CODM mutant selectively demethylates codeine. Use of this reengineered enzyme in the reconstitution of morphine biosynthesis could selectively disable a redundant pathway branch and therefore impact the yields of the downstream products codeine and morphine in subsequent metabolic engineering efforts.

INTRODUCTION

Opium poppy produces an array of medicinally important benzylisoquinoline alkaloids, including the analgesics codeine **10** and morphine **11** (Figure 1) (Facchini, 2001; Facchini et al., 2005). The biosynthesis of these alkaloids commences with the condensation of dopamine **1** and 4-hydroxyphenylacetaldehyde **2** to form (*S*)-norcoclaurine **3**, which is further modified to form (*S*)-reticuline **4**, the pivotal biosynthetic intermediate of all benzylisoquinoline alkaloids. (*S*)-reticuline **4** is subsequently converted to thebaine **5**, the intermediate at the entry point of the morphinan alkaloid pathway. Two biosynthetic routes have been proposed for the conversion of thebaine **5** to morphine **11** (Hagel and Facchini, 2010). In the first route (route A; see Figure 1), thebaine 6-O-demethylase (*Ps*T6ODM) demethylates thebaine **5** at the 6 position to form neopinone **7**, which spontaneously isomerizes to form codeinone **8**. Codeinone **8** is then enzymatically reduced to yield codeine **10**. Codeine O-demethylase (*Ps*CODM) demethylates codeine **10** at the 3 position to yield morphine **11**. Alternatively, in the second route (route B; see Figure 1), *Ps*CODM demethylates thebaine **5** at the 3 position to form oripavine **6**. *Ps*T6ODM catalyzes the second demethylation of oripavine **6**—this time at the 6 position—to form morphinone **9**, which is then reduced to form morphine **11**. Morphinan alkaloids thebaine **5**, oripavine **6**, codeine **10**, and morphine **11** all accumulate in *Papaver somniferum*, suggesting that both routes are operative in vivo (Facchini, 2001; Facchini et al., 2005). Here we demonstrate how exploiting natural enzyme variation through systematically mixing and matching the nonconserved amino acid regions of two demethylases (*Ps*CODM and *Ps*T6ODM) has led to an enzyme with new specificity: a *Ps*CODM mutant that is highly selective for codeine. The unique selectivity of the reengineered demethylase enzyme may allow us to explore how closing the metabolic valve of route B and redirecting substrate exclusively through route A (Figure 1) will impact downstream product yields in this branched natural product pathway.

RESULTS

Design of *P. somniferum Ps*CODM Mutants

A clustal alignment of *Ps*CODM, *Ps*T6ODM, and *Ps*DIOX2 (a *P. somniferum* 2-oxoglutarate/Fe(II)-dependent dioxygenase for which the native substrate has not yet been identified) revealed five specific regions where these dioxygenases differ significantly at the amino acid level: A_1 (residues 145–149), A_2 (residues 150–152), B (residues 334–336), C_1 (residues 338–342), and C_2 (residues 343 - 152). Lacking a crystal structure of a *P. somniferum* dioxygenase, we built a homology model of *Ps*CODM based on the crystal structure of *Arabidopsis thaliana* anthocyanidin synthase (*At*ANS), a structurally characterized 2-oxoglutarate/Fe(II)-dependent dioxygenase with moderate amino acid sequence similarity to *Ps*CODM (32% identity at the amino acid level) (Schwede et al., 2003; Wilmouth et al., 2002). We employed SWISS-MODEL, an automated protein homology-modeling server, to generate the model (Figure 2) (Schwede et al., 2003). Key residues likely to be involved in Fe(II)/2-oxoglutarate binding are highlighted in the Supplemental Information (Figure S1A available online). The five regions—grouped as follows, A_1 and A_2 (residues 145–152); B (residues 334–336); and C_1 and C_2 (residues 338–346)—were then mapped on to this homology model, where they appeared to be located proximal to the anthocyanin binding site (Figure 2).

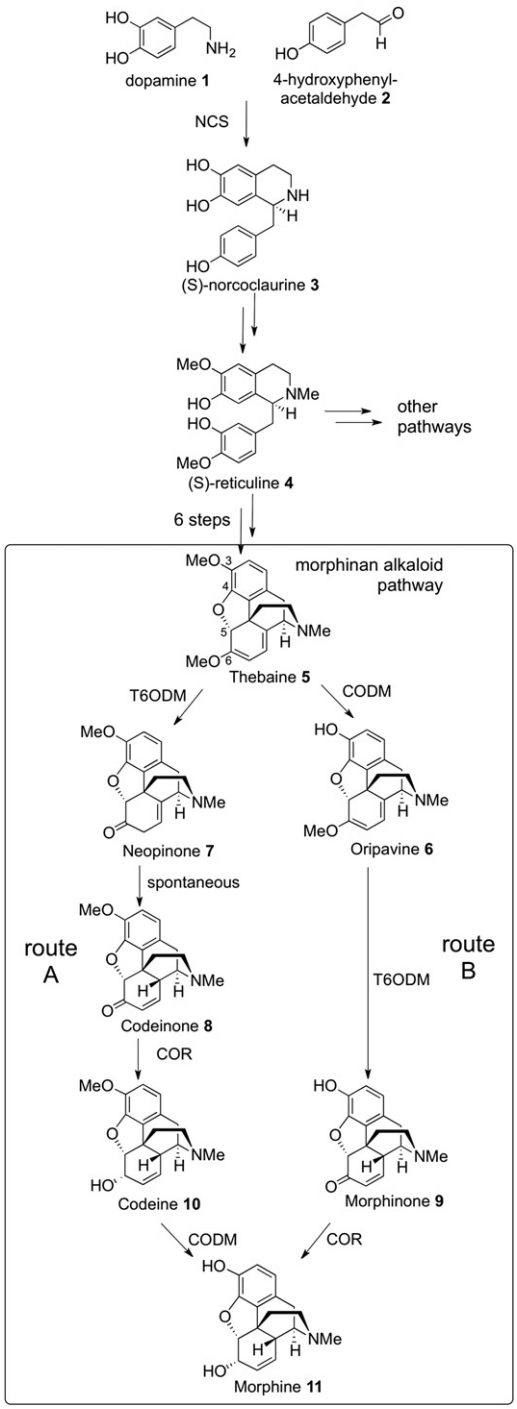

Figure 1. Biosynthesis of Benzylisoquinoline Alkaloids in *P. somniferum*

The biosynthetic pathways leading to morphine **11** via morphinone **9** and codeine **10**.

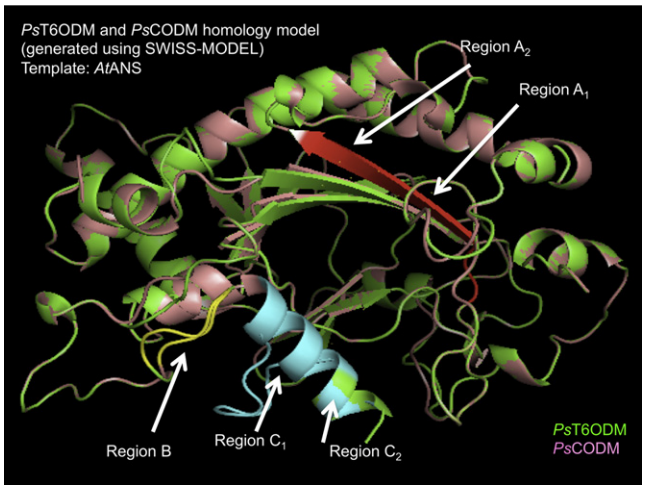

Figure 2. Homology Models of *Ps*T6ODM and *Ps*CODM Based on the Crystal Structure of *At*ANS

*Ps*T6ODM is indicated in green, and *Ps*CODM is indicated in pink. The models were created using SWISS-MODEL. Regions A_1 and A_2 (residues 145–152) are shown in red, B (residues 334–336) is in yellow, and C_1 and C_2 (residues 338–346) are in blue.

See also Figures S1, S2, S3, and S4 and Tables S1 and S2.

Initial protein expression screening revealed that all *Ps*T6ODM mutants are expressed at low levels. Therefore, in this study, we focused our efforts on developing engineered *Ps*CODM enzymes. We systematically replaced the native *Ps*CODM sequence with the corresponding sequence from *Ps*T6ODM at the five nonconserved regions using standard site-directed mutagenesis. In total, we constructed 16 *Ps*CODM mutants (Table 1).

Heterologous Expression of *P. somniferum Ps*CODM Mutants and In Vitro Activity Assay of *Ps*CODM Mutants

Dr. Jillian Hagel and Professor Peter Facchini (University of Calgary, Calgary, Alberta, Canada) provided *Escherichia coli* expression plasmids pQEDIOX1 and pQEDIOX3, which contain the open reading frames of *P. somniferum* T6ODM and CODM, respectively. Primers to design the mutant constructs are listed in the Supplemental Information (Table S1). We adapted heterologous expression conditions for *E. coli* from a previously reported protocol (Hagel and Facchini, 2010). Protein expression of the majority of *Ps*CODM mutants was robust (Figure S1B). Only the A_1A_2*BC_1C_2 mutant (S149M L151F S152T mutant; the asterisk designates the mutated region) was expressed at low levels, perhaps due to improper folding. We screened each of the mutant *Ps*CODM enzymes with substrates thebaine **10** and codeine **5** at a concentration of 0.25 mM. Detailed assay conditions are provided in the Experimental Procedures.

Product formation was monitored using liquid chromatography-mass spectrometry (LC-MS). LC-MS chromatograms of representative in vitro enzymatic assays of wild-type and mutant *Ps*CODM enzymes are shown in the Supplemental Information (Figure S2). These endpoint assays indicated that the majority of the mutants lost O-demethylase activity toward both thebaine **5** and codeine **10** substrates. Out of the total of 16 mutants, only two, A_1 A_2 B C_1* C_2 (E338G I340L L341V K342E) and A_1 A_2 B* C_1 C_2 (R334S R336S+T), retained O-demethylase activity toward either thebaine **5** or codeine **10** (Figure S2). The A_1 A_2 B* C_1 C_2 mutant was similar to the wild-type enzyme in that it turned over both thebaine **5** and codeine **10** to yield oripavine **6** and morphine **11**, respectively. The coelution of the wild-type

Table 1. *Ps*CODM Mutants that Were Constructed in This Study

	A_1	A_2	B	C_1	C_2 (Wild-type *Ps*CODM)
1	A_1*	A_2*	B	C_1*	C_2*
2	A_1*	A_2	B	C_1*	C_2*
3	A_1*	A_2*	B	C_1	C_2*
4	A_1*	A_2*	B	C_1*	C_2
5	A_1*	A_2*	B	C_1	C_2
6	A_1*	A_2	B	C_1	C_2*
7	A_1*	A_2	B	C_1*	C_2
8	A_1*	A_2	B	C_1	C_2
9	A_1	A_2*	B	C_1*	C_2*
10	A_1	A_2	B	C_1*	C_2*
11	A_1	A_2*	B	C_1	C_2*
12	A_1	A_2*	B	C_1*	C_2
13	A_1	A_2*	B	C_1	C_2
14	A_1	A_2	B	C_1	C_2*
15	A_1	A_2	B	C_1*	C_2
16	A_1	A_2	B*	C_1	C_2

An asterisk indicates that the residues in that region were mutated to those of PsT6ODM.

PsCODM and PsCODM A_1 A_2 B* C_1 C_2 mutant thebaine demethylation products suggests that the A_1 A_2 B* C_1 C_2 mutant retained regiospecificity for the 3 position of thebaine **5** (Figure S2). In contrast, the A_1 A_2 B C_1* C_2 mutant displayed only negligible O-demethylation activity for thebaine **5** but selectively turned over codeine **10** (Figure S2). Since codeine **10** only contains a methoxy group at the 3 position, the C3 regioselectivity of the A_1 A_2 B C_1* C_2 mutant is also clearly unchanged from the wild-type *Ps*CODM.

Competitive assay conditions with both thebaine **5** (0.25 mM) and codeine **10** (0.25 mM) were also employed to assess the activity of *Ps*CODM mutants (Figure 3). Morphine **11** and oripavine **6** products formed at a 4:1 ratio when wild-type *Ps*CODM was subjected to these assay conditions. Similarly, the A_1 A_2 B* C_1 C_2 mutant also yielded morphine **11** and oripavine **6** at approximately a 4:1 ratio, though notably at lower concentrations than the wild-type enzyme, indicating lower catalytic efficiency for the mutated enzyme. However, while the A_1 A_2 B C_1* C_2 mutant produced only negligible amounts of oripavine **6**, morphine **11** was produced at levels similar to those observed with wild-type enzyme, confirming the stringent selectivity of the A_1 A_2 B C_1* C_2 mutant.

Steady-State Kinetic Analyses of Wild-Type *P. somniferum* *Ps*CODM and Mutant $A_1A_2BC_1$*C_2

We measured the steady-state kinetic parameters of wild-type *Ps*CODM and mutant *Ps*CODM $A_1A_2BC_1$*C_2 by monitoring the rate of product formation. In total, we measured kinetic parameters for the following combinations: (1) wild-type *Ps*CODM with codeine (k_{cat}/K_M = 9.54 × 10^{-7} $s^{-1}\mu M^{-1}$ and K_M = 72.3 ± 33.4 μM); (2) wild-type *Ps*CODM with thebaine (k_{cat}/K_M = 1.52 × 10^{-8} $s^{-1}\mu M^{-1}$ and K_M = 216 ± 76.2 μM); and (3) *Ps*CODM mutant $A_1A_2BC_1$*C_2 with codeine (k_{cat}/K_M = 3.62x10^{-7} $s^{-1}\mu M^{-1}$ and K_M = 99.0 ± 22.4 μM). Notably, the mutant enzyme formed only negligible amounts of the thebaine demethylation product after 4 hr even when substrate concentrations were as high as 2,000 μM. Steady-state kinetic data are shown in the Supplemental Information (Figure S3 and Table S2).

DISCUSSION

Here we have altered the substrate specificity of *Ps*CODM, an enzyme involved in the biosynthesis of morphinan alkaloids. We identified regions for mutation by comparing three highly similar dioxygenases from *P. somniferum*, two of which have defined and distinct substrate and regioselective preferences. By scanning the aligned sequences we identified five nonconserved regions, A_1, A_2, B, C_1, and C_2 (Figure 2 and Figure S1A), that we speculated could confer either the substrate or regioselectivity of the dioxygenases in *P. somniferum*. To test this hypothesis, we systematically swapped the amino acid sequences of the A_1, A_2, B, C_1, and C_2 regions from thebaine 6 O-demethylase (*Ps*T6ODM) into *Ps*CODM. While most of the interchanges of these regions yielded *Ps*CODM mutants that were catalytically inactive, replacement of the C_1 region of *Ps*CODM with the C_1 region of *Ps*T6ODM led to a switch from a wild-type enzyme that accepts two substrates—thebaine **5** and codeine **10**—to a mutant enzyme that is selective for codeine **10** exclusively. This *Ps*CODM mutant, A_1 A_2 B C_1* C_2, contains only four amino acid changes from wild-type *Ps*CODM: E338G, I340L, L341V, and K342E.

Although structural information is not yet available for these demethylases, we could build a homology model for both wild-type and A_1 A_2 B C_1* C_2 mutant *Ps*CODM based on the anthocyanidin synthase enzyme docked with thebaine **5** (Figure S4). While these computational results must be interpreted with caution, docking studies suggest that the binding orientation of thebaine differs substantially between the wild-type enzyme and the A_1 A_2 B C_1* C_2 mutant (Figure S4). It is interesting that the homology model (Figure 2) also predicts that the C_1 region switches from an alpha helix in the wild-type enzyme to a random coil in the codeine-specific mutant, suggesting that the mutation in the C_1 region introduces changes to the *Ps*CODM secondary structure. The mutation in the C_1* region appears to prevent productive binding of the thebaine **5** substrate without greatly altering the catalytic efficiency for codeine **10** (k_{cat}/K_M = 9.54 × 10^{-7} $s^{-1}\mu M^{-1}$ for wild-type, k_{cat}/K_M = 3.62 × 10^{-7} $s^{1}\mu M^{-1}$ for mutant).

At the outset of this study, we hypothesized that the amino acid differences between *Ps*CODM, a C3 O-demethylase, and *Ps*T6ODM, a C6 O-demethylase, would control the distinct regioselectivity of the demethylation reactions. Therefore, we expected that swapping the non-conserved amino acid regions of these two enzymes would alter the regioselectivity of the mutated enzymes. However, the A_1 A_2 B C_1* C_2 *Ps*CODM mutant retained C3 regioselectivity. Instead, the mutations altered the substrate selectivity in an unpredictable manner. *Ps*T6ODM turns over thebaine **5** and oripavine **6**, and *Ps*CODM turns over thebaine **5** and codeine **10**. Despite both wild-type enzymes accepting thebaine **5**, the introduction of residues from *Ps*T6ODM into *Ps*CODM at the C_1 position (Figure 2) yields a mutant *Ps*CODM enzyme that is selective for codeine **10**. This change in substrate specificity does not readily correlate with the substrate specificity of the parent wild-type enzymes. Particularly in the absence of experimental structural data, it is difficult

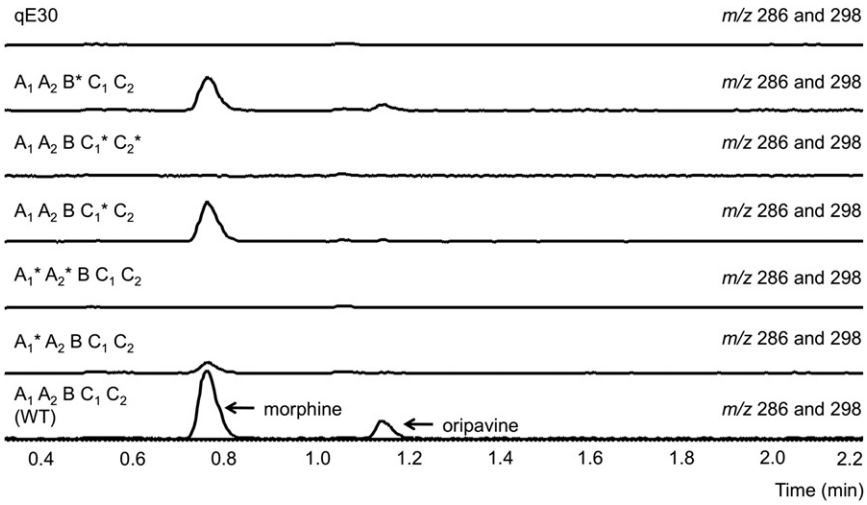

Figure 3. Biochemical Activity of PsCODM Enzymes

LC-MS traces of an in vitro enzymatic assay of wild-type and selected mutant PsCODM enzymes (1 μM final enzyme concentration) with 0.25 mM thebaine **5** and 0.25 mM codeine 10 in Tris buffer (100 mM Tris-HCl, 10% [v/v] glycerol, 14 mM 2-mercaptoethanol, pH 7.4) containing 10 mM 2-oxoglutarate, 10 mM sodium ascorbate and 0.5 mM iron (II) sulfate. Reactions were performed at 30°C for 4 hr. Mass-to-charge ratio (m/z) 286 corresponds to morphine **11**; m/z 298 corresponds to oripavine **6**. LC-MS spectra are normalized to the same y axis scale.

See also Figures S1, S2, S3, and S4 and Tables S1 and S2.

to rationalize what structural changes these mutations confer to *Ps*CODM and how these changes impact substrate specificity. Nevertheless, while this work highlights the difficulty of rational, structure-based protein design, we successfully demonstrate how sequence alignment of enzymes with subtle differences in specificity can be used to readily generate swapped sequences that are functionally distinct from naturally occurring wild-type variations.

One goal of metabolic engineering is the removal of shunt or redundant pathways that adversely impact production yields of a desired compound (Pickens et al., 2011). This A_1 A_2 B C_1* C_2 *Ps*CODM mutant may fulfill an engineering function by providing a means to shut off a redundant route (route B in Figure 1) in morphinan biosynthesis. Because A_1 A_2 B C_1* C_2 *Ps*CODM fails to demethylate thebaine **5** to form oripavine **6**, the first committed step of route B, replacement of wild-type *Ps*CODM with the A_1 A_2 B C_1* C_2 mutant would presumably force the morphine pathway to proceed via route A. Notably, growers in India, a major cultivator of licit opium, inadvertently counterselected for *P. somniferum* cultivars low in oripavine **6** when selecting for the highest seed quality and opium yields (Prajapati et al., 2002), suggesting that low oripavine **6** production levels may correlate with economically desirable traits. Therefore, in addition to assessing how knockouts of wild-type *Ps*CODM and *Ps*T6ODM affect flux into morphine production, it will be of interest to observe how using the *Ps*CODM A_1 A_2 B C_1* C_2 mutant—which effectively sidesteps oripavine 6 production by committing thebaine **5** to route A—instead of the wild-type *Ps*CODM enzyme would impact titers of codeine **10** and morphine **11** (Prajapati et al., 2002). Moreover, substantial interest lies in reconstituting morphinan alkaloid biosynthesis in yeast and *E. coli* (Hawkins and Smolke, 2008; Minami et al., 2008; Nakagawa et al., 2011). Mutants with altered specificity such as *Ps*CODM A_1 A_2 B C_1* C_2 could provide important building blocks for these synthetic biology efforts.

SIGNIFICANCE

We have altered the substrate specificity of a morphinan pathway enzyme codeine O-demethylase (*Ps*CODM). One *Ps*CODM mutant, mutant A_1 A_2 B C_1* C_2 (E338G I340L L341V K342E), exhibits demethylase activity exclusively toward codeine 10, whereas the wild-type *Ps*CODM exhibits demethylase activity with both codeine 10 and thebaine 5. These results provide a starting point for rationalizing how *Ps*CODM and *Ps*T6OD, two enzymes involved in morphinan biosynthesis with 73% identity at the amino acid level, facilitate O-demethylation regioselectivity on separate sets of substrates. In addition to providing insight into O-demethylase substrate selectivity, this mutant could also be useful in biotechnological efforts to provide *P. somniferum* strains with augmented yields of codeine 10 and morphine 11 and diminished titers of oripavine 6, an intermediate in a redundant pathway branch that has been associated with poor seed quality and low opium yields. In short, mutants with enhanced enzyme selectivity will allow us to explore how the targeted disruption of a redundant pathway branch affects downstream product yields and may enable more efficient production of these high value compounds. In addition to the potential biotechnological applications of this enzyme, these protein engineering efforts also provide a starting point for understanding how the subtle sequence differences of highly similar enzymes can impact substrate and regioselectivity.

EXPERIMENTAL PROCEDURES

Construction of *Ps*CODM Mutant Expression Plasmids

pQEDIOX1 (pQET6ODM) and pQEDIOX3 (pQECODM), which contain the open reading frames of *Ps*T6ODM and *Ps*CODM, respectively, were provided by Professor Peter Facchini and Dr. Jillian Hagel (University of Calgary). To obtain the 16 CODM mutants (Table 1), site-directed mutagenesis (SDM) was performed using the Stratagene QuikChange Site-Directed Mutagenesis kit. SDM primers are listed in the Supplemental Information (Table 1). The *Ps*CODM mutant constructs were sequenced to verify the DNA sequence and were subsequently transformed for expression into *E. coli* strain SG13009 (QIAGEN) via electroporation using standard protocols.

Heterologous Expression of *Ps*CODM Mutants

A single transformed *E. coli* colony (strain SG13009 [QIAGEN]) was inoculated in 10 ml Luria-Bertani (LB) media supplemented with kanamycin (0.05 g/l) and ampicillin (0.1 g/l) and incubated overnight at 37°C with shaking at 225 rpm.

Subsequently, 800 ml LB media supplemented with kanamycin (0.05 g/l) and ampicillin (0.1 g/l) was inoculated with an overnight culture (8 ml) and incubated at 37°C with shaking at 225 rpm until reaching an optical density 600 (OD_{600}) of 0.6. Protein expression was induced by the addition of isopropyl β-D-galactopyranoside (IPTG; final concentration 0.3 mM). Following induction, cells were incubated at 6°C with shaking at 225 rpm for 24 hr. Cells were harvested by centrifugation and lysed by sonication. The hexa-histidine-tagged *Ps*CODM mutants were purified using Talon colbalt affinity column (Clontech) using the manufacturer's protocols. Eluted enzyme was subsequently buffer-exchanged into Tris buffer (100 mM Tris-HCl, pH 7.4, 10% [v/v] glycerol, and 14 mM 2-mercaptoethanol) and immediately assayed for activity. These enzymes were not stable upon extended storage.

In Vitro Activity Assay of *Ps*CODM Mutants

The in vitro activity assay protocol was adapted from a previous report (Hagel and Facchini, 2010). Briefly, the assay for 2-oxoglutarate/Fe(II)-dependent dioxygenase activity was performed using a 100 μl reaction mixture of 100 mM Tris-HCl (pH 7.4), 10% (v/v) glycerol, 14 mM 2-mercaptoethanol, 0.25 mM alkaloid(s), 10 mM 2-oxoglutarate, 10 mM sodium ascorbate, 0.5 mM $FeSO_4$, and 1 μM purified enzyme. Assays were carried out for 4 hr at 30°C. Aliquots (25 μl) were quenched in 1 ml methanol containing yohimbine (500 nM) as an internal standard. The samples were centrifuged in a microcentrifuge (13,000 rpm, 5 min) to remove particulates and then analyzed by LC-MS. Samples were ionized by ESI with a Micromass LCT Premier TOF Mass Spectrometer. The LC was performed on an Acquity Ultra Performance BEH C18, 1.7 μm, 2.1 × 100 mm column on a gradient of 10%–90% acetonitrile/water (0.1% formic acid) over 5 min at a flow rate of 0.6 ml/min. The appearance of morphine **11** and oripavine **6** was monitored by peak integration and normalized to the internal standard. All chemicals were obtained from a commercial source (Sigma Aldrich).

Steady-State Kinetic Assay of Wild-Type CODM and A_1 A_2 B C_1* C_2 Mutant

Assay components were used in the following final concentrations: pH 7.4 Tris-HCl (67 mM) containing 10% (v/v) glycerol and 14 mM 2-mercaptoethanol, α-ketoglutarate (6.7 mM), sodium ascorbate (6.7 mM), iron (II) sulfate (333 μM), and enzyme wild-type (4.1 μg/ml) or Enzyme Mutant (18 μg/ml), in an assay volume of 150 μl. The enzyme concentrations were estimated by Bradford assay. Assays were initiated by addition of iron sulfate and conducted at 30°C. Aliquots (25 μl) were quenched every 30 min from 1 to 3 hr with 975 μl methanol containing 500 nM ajmaline as an internal standard. Prior to analysis, methanol quenched samples were centrifuged in a microcentrifuge at 13,000 rpm for 5 min to remove any particulates. Liquid chromatography was performed on an Acquity Ultra Performance BEH C18, 1.7 μm, 2.1 × 100 mm column. The gradient was 10%–90% acetonitrile over 4 min with water and 0.1% formic acid in water as the second solvent. The flow rate was 0.5 ml/min. We performed electrospray ionization (ESI) with a Micromass LCT Premier TOF Mass Spectrometer in positive ionization V-mode.

Product accumulation was measured to determine the kinetic parameters. A standard curve for morphine, the demethylation product of codeine, was constructed to determine the kinetic parameters of codeine demethylation. However, oripavine, the demethylation product of thebaine, was unavailable; therefore, hydromorphonone, which was available, was used as a surrogate. Plotted experimental data were fit to a Michaelis-Menten curve using SigmaPlot version 9.0. Experiments were duplicated or triplicated to ensure reproducibility (Table S2).

SUPPLEMENTAL INFORMATION

Supplemental Information includes four figures and two tables and can be found with this article online at doi:10.1016/j.chembiol.2012.04.017.

ACKNOWLEDGMENTS

We thank Dr. Jillian Hagel and Professor Peter Facchini (University of Calgary) for providing *E. coli* expression plasmids pQEDIOX1 and pQEDIOX3, which contain the open reading frames of PsT6ODM and CODM, respectively, as well as for helpful discussions. W.S.G. gratefully acknowledges a National Science Foundation predoctoral fellowship. Funding was provided by the John Innes Centre, and start-up funds were provided by the University of East Anglia. S.O.C. is supported by a Synergy faculty position at the John Innes Centre and the University of East Anglia.

Received: March 21, 2012
Revised: April 18, 2012
Accepted: April 23, 2012
Published: June 21, 2012

REFERENCES

Facchini, P.J. (2001). Alkaloid biosynthesis in plants: Biochemistry, cell biology, molecular regulation and metabolic engineering applications. Annu. Rev. Plant Physiol. Plant Mol. Biol. *52*, 29–66.

Facchini, P.J., Bird, D.A., Bourgault, R., Hagel, J.M., Liscombe, D.K., MacLeod, B.P., and Zulak, K.G. (2005). Opium poppy: a model system to investigate alkaloid biosynthesis in plants. Can. J. Bot. *83*, 1189–1206.

Hagel, J.M., and Facchini, P.J. (2010). Dioxygenases catalyze the O-demethylation steps of morphine biosynthesis in opium poppy. Nat. Chem. Biol. *6*, 273–275.

Hawkins, K.M., and Smolke, C.D. (2008). Production of benzylisoquinoline alkaloids in Saccharomyces cerevisiae. Nat. Chem. Biol. *4*, 564–573.

Minami, H., Kim, J.-S., Ikezawa, N., Takemura, T., Katayama, T., Kumagai, H., and Sato, F. (2008). Microbial production of plant benzylisoquinoline alkaloids. Proc. Natl. Acad. Sci. USA *105*, 7393–7398.

Nakagawa, A., Minami, H., Kim, J.S., Koyanagi, T., Katayama, T., Sato, F., and Kumagai, H. (2011). A bacterial platform for fermentative production of plant alkaloids. Nat Commun. *2*, 326.

Pickens, L.B., Tang, Y., and Chooi, Y.-H. (2011). Metabolic engineering for the production of natural products. Annu. Rev. Chem. Biomol. Eng. *2*, 211–236.

Prajapati, S., Bajpai, S., Singh, D., Luthra, R., Gupta, M.M., and Kumar, S. (2002). Alkaloid profiles of the Indian land races of the opiumpoppy Papaver somniferum L. Genet. Resour. Crop. Evol. *49*, 183–188.

Schwede, T., Kopp, J., Guex, N., and Peitsch, M.C. (2003). SWISS-MODEL: An automated protein homology-modeling server. Nucleic Acids Res. *31*, 3381–3385.

Wilmouth, R.C., Turnbull, J.J., Welford, R.W., Clifton, I.J., Prescott, A.G., and Schofield, C.J. (2002). Structure and mechanism of anthocyanidin synthase from Arabidopsis thaliana. Structure *10*, 93–103.

